Analysis, Design, and Actual Fabrication of a Hybrid Microstrip-SIW Bandpass Filter Based on Cascaded Hardware Integration at X-Band

Kemal Guvenli[1, 2, *], Sibel Yenikaya[2], Mustafa Secmen[3]
[1]*Department of Electronics and Automation, Hitit University, Kuzey Kampusu, 19030 Corum, Turkey*
[2]*Department of Electrical and Electronics Engineering, Bursa Uludag University, Gorukle Kampusu, 16059 Nilufer, Bursa, Turkey*
[3]*Department of Electrical and Electronics Engineering, Yasar University, Universite Cad., No: 37-39, Agacli Yol, 35030, Bornova, Izmir, Turkey*
kemalguvenli@hitit.edu.tr

***Abstract*—In this paper, the Microstrip-Substrate Integrated Waveguide (M-SIW) bandpass filter is designed, simulated, and fabricated based on the theoretical analysis. The Substrate Integrated Waveguide (SIW) highpass filter and the microstrip lowpass filter are combined in a hybrid design to achieve the M-SIW bandpass filter in the X-band. This design is more comprehensible and easier to achieve a bandpass filter at a desired frequency. The SIW highpass filter and the microstrip lowpass filter are connected in series to achieve the bandpass filter. To the measured results of the fabricated M-SIW bandpass filter, the center frequency is 10.20 GHz and the bandwidth is 2.40 GHz. When the analytical and measurement results are compared, the frequency change in the cut-off frequency is 6.02 % and the frequency change in the bandwidth is 8.74 %. It is generally seen that analytical, simulation, and measurement results are compatible with each other. The M-SIW bandpass filter can be broadly used in radar, Worldwide Interoperability for Microwave Access (WiMAX), and satellite technologies. The filters are simulated in Computer Simulation Technology (CST) Studio Suite.**

***Index Terms*—Bandpass filter; Cascaded integration; Substrate integrated waveguide; Microstrip.**

I. INTRODUCTION

Microwave filters play an important role in today's communication technology [1]. Especially in the fifth generation (5G), wireless communication technologies with high communication speed, microwave filters have a more important place [2]. In addition, satellite technologies are developed rapidly in line with increasing demand. Furthermore, microwave filters have a wide range of applications in satellite [3], Machine-to-Machine (M2M), and radar technologies [4].

Substrate Integrated Waveguide (SIW) has a lower-cost, simple integration, and planar structure compared to rectangular waveguides, but it has a greater loss and lower Q-factor. SIW structures, which act as highpass filters, are used in filter design due to their mentioned properties [5]. Different structures are used to obtain a bandpass filter in some of the previous studies, such as microstrip structure [5], air-filled structure [6], symmetric inductive post structure [7], resonator structure [8], bent structure [9], Low Temperature Co-fired Ceramics (LTCC) structure [10], Through-Silicon Via (TSV) structure [11], cross-coupled structure [12], perturbed circular cavity structure [13], Fourier-varying via-vole walling structure [14], and GaAs-based chip filter structure [15], [16]. As the microstrip structure is easier, cheaper, and more comprehensible, it is preferred for the lowpass filter section of the bandpass filter [17].

The main purpose of this study is to design a modular expandable bandpass filter that can be a reference for future studies. The hybrid bandpass filter is designed in three stages. In the first step, a highpass filter is designed. In the second step, a lowpass filter is designed. In the third step, a substrate integrated waveguide highpass filter and a microstrip lowpass filter are combined in a hybrid filter design. The M-SIW bandpass filter with the desired bandwidth and cut-off frequency is obtained by cascaded hardware integration of these two filter designs. This hybrid design approach helps to produce the bandpass filter transparently and quickly. Simple and clear structures are preferred instead of complex structures. Thus, the bandpass filter with desired cut-off frequency and bandwidth can be designed with fewer variables. This method increases the flexibility of the bandpass filter design.

The lengths of the microstrip lowpass filter parameters are determined based on $0.125\lambda_{lpf}$ (λ_{lpf} is the wavelength of the microstrip lowpass filter). The transition from microstrip to SIW is a tapered section [18]. Frequency response of full-mode SIW is better than the transmission efficiency of half-mode SIW. Therefore, full-mode SIW is preferred in this bandpass filter design [19].

II. ANALYSIS AND DESIGN OF THE PROPOSED M-SIW BANDPASS FILTER

In this study, the frequency range of the proposed M-SIW bandpass filter is considered 8.39 GHz–11.02 GHz. The

Manuscript received 11 August, 2020; accepted 23 December, 2020.

center frequency f_C is 9.62 GHz, the -3 dB lower cut-off frequency f_L = 8.58 GHz, the high cut-off frequency f_H = 11.2 GHz, and the bandwidth BW = 2.63 GHz. The M-SIW bandpass filter is achieved by using a lowpass filter and a highpass filter structures [20], [21]. Firstly, the cut-off frequencies of the lowpass and highpass filters should be determined. In this way, it is possible to get the appropriate bandwidth for a desired cut-off frequency of bandpass filter [20]–[22].

A. *First Step: The SIW Highpass Filter Design*

SIW mainly performs as a planar rectangular waveguide. A planar rectangular waveguide is a highpass filter [21], [22].

The geometry and parameters of the SIW highpass filter are shown in Fig. 1. The Rogers 4003C substrate material is used in filter design (h = 1.52 mm, ϵ_r = 3.38, and tanδ = 0.0027) [20], [23].

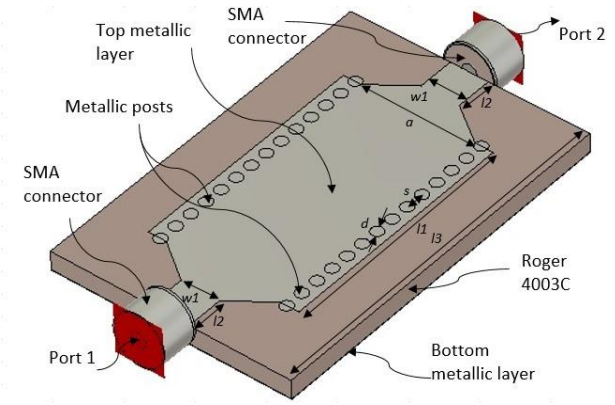

Fig. 1. The geometry of the SIW highpass filter (Top view).

The lengths of parameters of the SIW highpass filter are shown in Table I.

TABLE I. PARAMETERS AND LENGTHS OF THE HIGHPASS SIW FILTER.

Parameter	Length	Parameter	Length
d	1 mm	l_1	19.5 mm
a	9.5 mm	l_2	3 mm
h	1.52 mm	l_3	30 mm
s	1.5 mm	w_1	3.2 mm

The dominant TE mode of a planar rectangular waveguide is TE_{10} (m = 1, n = 0) mode. The wavelength of the SIW highpass filter (λ_{hpf}) is calculated as 18.983 mm according to (1), (2). Besides, the CST Studio Suite simulation results of the SIW highpass filter from 6 GHz to 16 GHz are shown in Fig. 2.

$$fc_{mn} = [1/(2 \times \pi \times \sqrt{(\mu \times \varepsilon)})] \times \times [((m \times \pi)/a)^2 + ((n \times \pi)/b)^2]^{1/2}, \quad (1)$$

$$\lambda = c/(f \times \sqrt{\varepsilon_r}). \quad (2)$$

As shown in Fig. 2, out-of-band frequency suppression is observed to be good in the simulation solution. It is seen that there is a sharp transition-band in the simulation results. The SIW highpass filter has a good "insertion loss" (IL) performance. However, within the frequency band (pass-band) from 13.5 GHz to 14.5 GHz, the "return loss" (RL) performance of the SIW highpass filter is a little poor. The cut-off frequency f_C is 8.06 GHz in the simulation results. Based on the simulation results, it is seen that the high pass filter design is good.

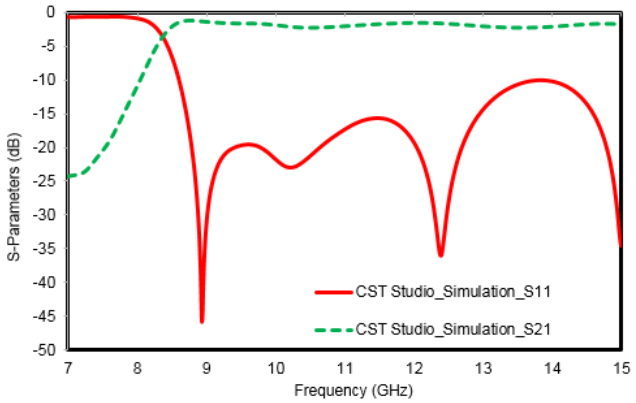

Fig. 2. The simulation results of the SIW highpass filter.

B. *Second Step: The Microstrip Lowpass Filter Design*

An easy way to design a microstrip lowpass filter is to use alternative sections that are part of a very high or very low characteristic impedance line. These filters are often described as stepped-impedance because of a good performance of group delay. Therefore, we prefer to use the stepped impedance method to design a microstrip lowpass filter [17], [24]. The Rogers 4003C substrate material is used in filter design.

The geometry and parameters of the microstrip lowpass filter are shown in Fig. 3.

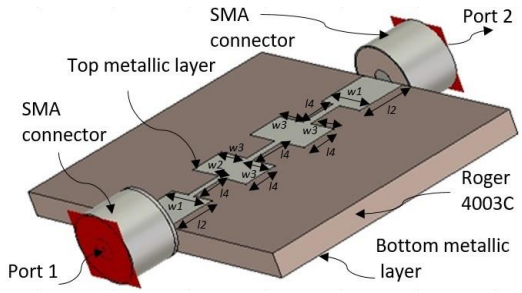

Fig. 3. The geometry of the microstrip lowpass filter (Top view).

The values of the microstrip lowpass filter's parameters are shown in Table II.

TABLE II. PARAMETERS AND LENGTHS OF THE MICROSTRIP LOWPASS FILTER.

Parameter	Length	Parameter	Length
w_1	3.2 mm	l_2	3 mm
w_2	0.44 mm	l_3	30 mm
w_3	1.9 mm	l_4	1.9 mm
h	1.52 mm		

The microstrip lowpass filter is designed by using the Insertion Loss Method. The element values of the equivalent electrical circuit of microstrip lowpass filter are theoretically calculated (R_0 = 50 Ω, N = 6). The circuit elements of the microstrip lowpass filter are C_1 = 0.1471 pF, L_2 = 1.0053 nH, C_3 = 0.5493 pF, L_4 = 1.3732 nH, C_5 = 0.1177 pF, and L_6 = 0.3679 nH. The equivalent electrical circuit of the microstrip lowpass filter is shown in Fig. 4(a). The wavelength (λ_{lpf}) of the microstrip lowpass filter is

calculated as 11.697 mm. Furthermore, the microstrip lowpass filter response between 7 GHz and 15 GHz in CST Studio Suite simulation and analytical results are shown in Fig. 4(b).

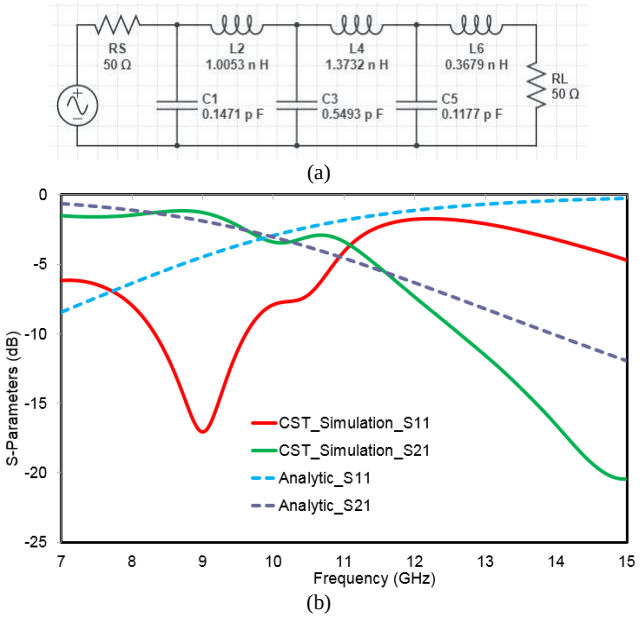

Fig. 4. The microstrip lowpass filter: a) equivalent electrical circuit (Chebyshev); b) the simulated and analytical results of the microstrip lowpass filter.

As shown in Fig. 4(b), the out-of-band frequency suppression in the simulation is similar to the analytical solution. It is clearly seen that there is a wide transition-band in analytical and simulation solutions. The cut-off frequency, f_C, is 12.62 GHz in the simulation and 13.94 GHz in the analytic results. Based on theoretical calculations, the frequency change in f_C is 7.17 %. However, within the frequency band (pass-band) from 7 GHz to 8.5 GHz, the "return loss" (RL) performance of the microstrip lowpass filter is a little poor. The microstrip lowpass filter has a good "insertion loss" (IL) performance generally. According to all results, it is seen that the low pass filter design is good.

C. *Third Step: The M-SIW Bandpass Filter Design*

The geometry and parameters of the M-SIW bandpass filter with two ports are shown in Fig. 5.

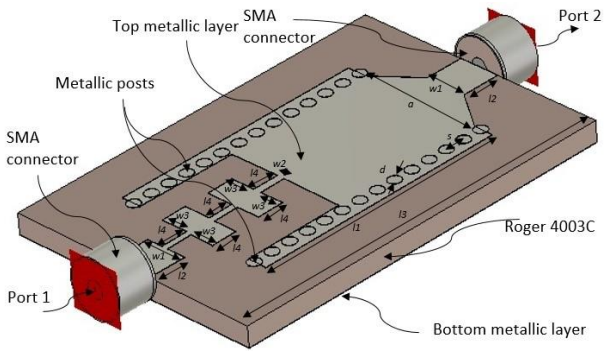

Fig. 5. The geometry of the M-SIW bandpass filter (Top view).

The lengths of parameters of the M-SIW bandpass filter are shown in Table III.

TABLE III. PARAMETERS AND LENGTHS OF THE M-SIW BANDPASS FILTER.

Parameter	Length	Parameter	Length
a	9.5 mm	w_3	1.9 mm
d	1 mm	l_1	19.5 mm
h	1.52 mm	l_2	3 mm
s	1.5 mm	l_3	30 mm
w_1	3.2 mm	l_4	1.9 mm
w_2	0.44 mm		

The following equations are used for Bandpass Filter Transformations [17]:

– The center frequency, ω_0

$$\omega_0 = \sqrt{(\omega_1 \times \omega_2)}. \quad (3)$$

– The fractional bandwidth of the pass-band

$$\Delta = (\omega_2 - \omega_1)/\omega_0. \quad (4)$$

– A series inductor (L_k) is converted to L'_k and C'_k (Series LC circuit):

$$L'_k = L_k/(\Delta\omega_0), \quad (5)$$
$$C'_k = \Delta/(\omega_0 \times L_k). \quad (6)$$

– A shunt capacitor (C_k) is converted to L'_k and C'_k (Shunt LC circuit):

$$L'_k = \Delta/(\omega_0 \times C_k), \quad (7)$$
$$C'_k = C_k/(\Delta\omega_0). \quad (8)$$

The Insertion Loss Method is applied in this bandpass filter design. The element values of the equivalent electrical circuit of the bandpass filter are theoretically calculated (N = 6 and R_0 = 50 Ω).

The circuit elements of the M-SIW bandpass filter are C_1 = 0.1678 pF, L_1 = 1.5732 nH, C_2 = 1.719 pF, L_2 = 0.1535 nH, C_3 = 0.044 pF, L_3 = 5.871 nH, C_4 = 2.348 pF, L_4 = 0.1124 nH, C_5 = 0.0614 pF, L_5 = 4.298 nH, C_6 = 0.629 pF, and L_6 = 0.419 nH. The circuit of the M-SIW bandpass filter is shown in Fig. 6.

The wavelength (λ_{bpf}) of the M-SIW bandpass filter is calculated as 11.69 mm by using (1), (2). The pass-band is 2.63 GHz. In addition, the comparison of the analytical and simulation results is given in Fig. 6(b). The value of BW is 2.63 GHz in the analytical solution, and it is 3.30 GHz in the simulation solution. In general, the out-of-band frequency suppression in the simulation is close to the analytical results. The center frequency, f_C, is 10.61 GHz in the simulation, and it is 9.62 GHz in the analytical solution.

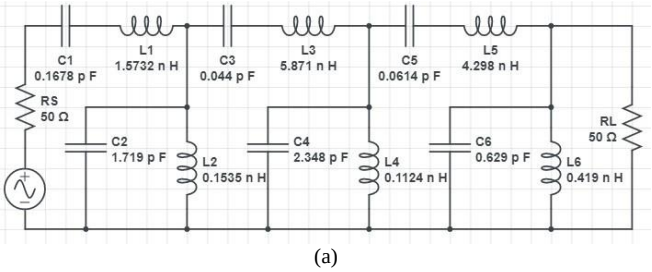

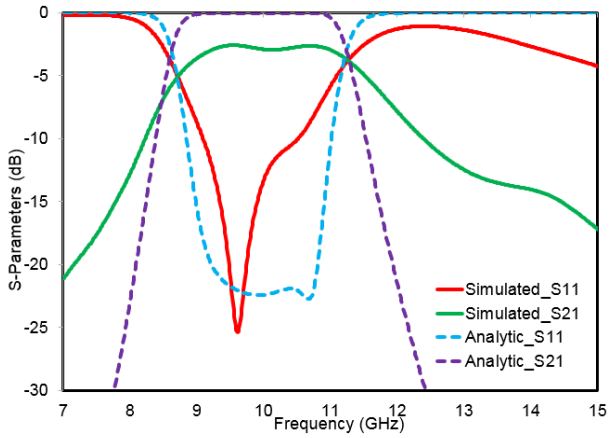

(b)

Fig. 6. The M-SIW bandpass filter: a) equivalent electrical circuit (Chebyshev); b) the simulated and analytical results.

III. EXPERIMENTAL VERIFICATION AND MEASUREMENT RESULTS

A Computer Numerical Control (CNC) milling machine is used for filter production. The M-SIW bandpass filter, which is fabricated by using the Rogers 4003C material, is shown in Fig. 7(a) and Fig. 7(b).

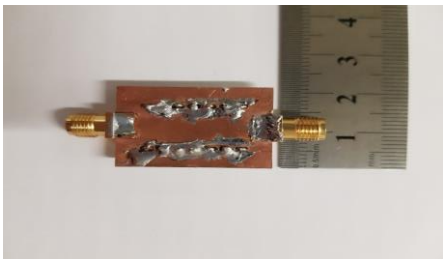

(a)

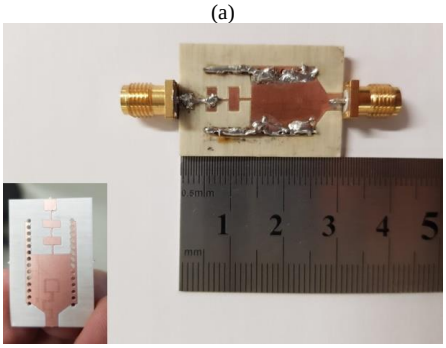

(b)

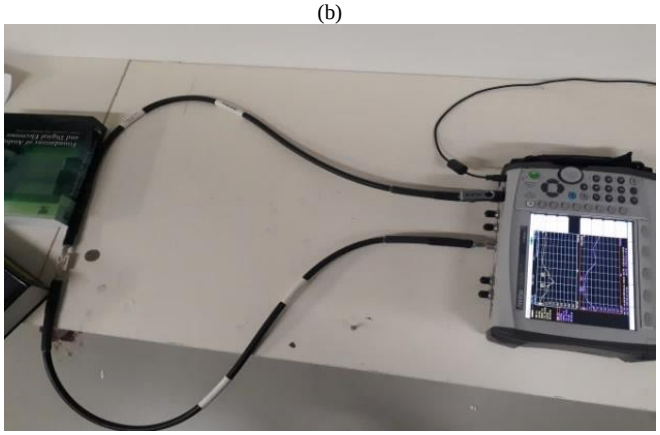

(c)

Fig. 7. The fabricated M-SIW bandpass filter: a) Bottom view; b) Top view; c) the experimental measurement.

The conductive copper wire with a thickness of 1 millimeter is passed through the holes of the SIW filter and it is soldered to the material.

The M-SIW bandpass filter is measured by using the Anritsu handheld vector network analyzer (VNA Master MS2028C) in Antenna and Microwave Lab. of Electrical and Electronic Engineering Dept. at Yasar University. The M-SIW bandpass filter is measured on 4001 points of the frequency range (sampling rate is 10 kHz; the whole frequency band is from 7 GHz to 15 GHz). The M-SIW bandpass filter in the measurement is represented in Fig. 7(c).

The simulated and measured results of the M-SIW bandpass filter are given in Fig. 8. As shown in Fig. 8, the out-of-band frequency suppression in measurement is as good as in simulation. At the same time, the frequency response in the pass-band is close to each other in both simulation and measurement results. The bandwidth in the simulation is 3.30 GHz. The center frequency, f_C, is 10.61 GHz in the simulation.

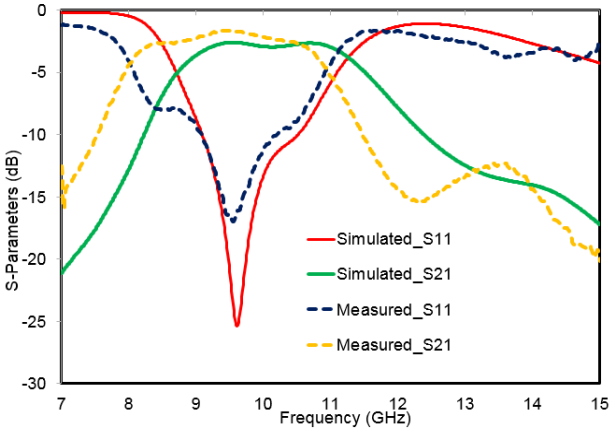

Fig. 8. The simulated and measured results of the M-SIW bandpass filter.

According to the results of the measurement shown in Fig. 8, the bandwidth of the M-SIW bandpass filter is 2.40 GHz. The -3dB lower cut-off frequency (f_L) is 9.08 GHz, the -3dB upper cut-off frequency (f_H) is 11.48 GHz, and the center frequency (f_C) is 10.20 GHz. The "return loss" (RL) is commonly greater than 10 dB in the measured pass-band. In addition, the "insertion loss" (IL) is less than 3 dB in the measured pass-band.

Analytical, simulated, and measured values are provided in Table IV.

The fabricated bandpass filters with some previous Microstrip-SIW, SIW, Complementary Split Ring Resonators (CSRRs)-SIW, and Spoof Surface Plasmon Polaritons (SSPPs)-SIW are compared with measured performance and type of design in Table V. It is shown that the bandpass filters in [21] and [25] have a very wide pass-band. The filters in "this work" and [18] have approximately the same "insertion loss" (IL) and "return loss" (RL). The filter in [19] has a very narrow pass-band. However, its "insertion loss" (IL) seems to be the best among them. The filters with different cut-off frequency in "this work" and in [9] have similar BW.

TABLE IV. THE RESULTS OF ANALYSIS, SIMULATION, AND MEASUREMENT OF THE M-SIW BANDPASS FILTER.

Operation	-3 dB Lower Cut-off Frequency (f_L) (GHz)	Center Frequency (f_C) (GHz)	-3 dB Upper Cut-off Frequency (f_H) (GHz)	Bandwidth (BW) (GHz)
Analysis	8.39	9.62	11.02	2.63
Simulation	9.09	10.61	12.39	3.30
Measurement	9.08	10.20	11.48	2.40

TABLE V. THE COMPARISON OF BANDPASS SIW FILTER DESIGNS.

Ref.	Type of Design	Center Freq./BW* (GHz)	S_{11}* (dB)	S_{21}* (dB)	Ɛr*/tanδ*	*Size (mm × mm)*
[9]	Full-mode and CSRR-SIW	(5.5–8.25)**/2.75	> 16.5	< 2	3.55/0.0023	59×17.2
[18]	Half-mode and Microstrip-SIW	12.85/9.50	> 10	< 1.4	2.2/0.0013	76×7.1
[19]	Half-mode and Microstrip-SIW	(7.10–7.20)**/0.1	> 22	< 2	2.2/0.0013	123×11.2
[21]	Full-mode and SIW	30.83/20	> 15	< 1.5	3/0.001	28.8×11.5
[25]	Half-mode and SSPs-SIW	(15.6–32.1)**/16.5	> 10	< 0.8	2.65/0.0015	80×10
This work	Full-mode and Microstrip-SIW	10.20/2.40	> 10	< 3	3.38/0.0027	30×20

*Notes: *BW, S_{11}, S_{21}, tanδ, and Ɛr mean bandwidth, return loss, insertion loss tangent, and dielectric constant.*
***Since the center frequency is not given, the pass-band is written.*

IV. DISCUSSION

According to the hybrid M-SIW bandpass filter results, the center frequency is 9.62 GHz in analysis, 10.61 GHz in simulation, and 10.20 GHz in measurement. The bandwidths of the M-SIW bandpass filter are 2.63 GHz, 3.30 GHz, and 2.40 GHz, respectively.

The result of the S-parameter of the M-SIW filter depends on the diameter of the SIW's embedded metallic post, connector loss, and soldering errors. Therefore, such problems may cause bandwidth deflection according to Table IV. Comparison results between the proposed M-SIW bandpass filter and several manufactured bandpass filters based on SIW are presented in Table V. It is seen that the size of the designed full-mode M-SIW filter (20 mm × 30 mm) is smaller compared to SIW filters for X-band applications.

The hybrid design approach (one inside another) is applied to highpass and lowpass filters' structure based on 0.125λ. This approach is used in the lowpass structure to improve the bandpass filter responses. The measured "return loss" (RL) is generally greater than 10 dB, and the measured "insertion loss" (IL) is less than 3 dB on the pass-band. The performance of the M-SIW bandpass filter is satisfactory as represented in the RL and IL results. Similar to analytical results, the out-of-band frequency suppression is found to be satisfactory in both measurement and simulation. The simulated bandwidth (BW) of the M-SIW bandpass filter is 3.30 GHz and the measured BW is 2.40 GHz. The reason for the low BW in the measurement results compared to the simulation is thought to be due to the manufacture of the M-SIW bandpass filter.

V. CONCLUSIONS

In this study, the theory and hybrid design of the bandpass filter, which has a cascaded structure, are discussed. Unlike the design of the conventional bandpass filter, the M-SIW bandpass filter is clearly presented as a combination of the microstrip lowpass and SIW highpass filters. The period of filter design is shortened and the lowpass/highpass filter effects are clearly seen with this hybrid method. Thus, the bandpass filter can be designed and implemented easily for the desired frequency range. The Rogers 4003C material is seen to be a proper substrate for the application of the M-SIW bandpass filter. With the Rogers 4003C material, successful results can be obtained in the C-band, as well as in the X-band. However, it is predicted that losses will increase in the Ku-band.

It is concluded that analysis, simulation, and measurement values were found to be consistent with each other. By using this cascaded hardware integration, it is also possible to design new bandpass filters having different cut-off frequency. It is evident that the sensitivity of the CST Studio Suite simulation program based on the Finite Integration Technique (FIT) is satisfactory [26], [27].

CONFLICTS OF INTEREST

The authors declare that they have no conflicts of interest.

REFERENCES

[1] L. Huang and N. Yuan, "A compact wideband SIW bandpass filter with wide stopband and high selectivity", *Electronics*, vol. 8, no. 4, p. 440, 2019. DOI: 10.3390/electronics8040440.

[2] J. Li, Y. Huang, H. Wang, P. Wang, and G. Wen. "38-GHz SIW filter based on the stepped-impedance face-to-face E-shaped DGSs for 5G application", *Microwave and Optical Technology Letters*, vol. 61, no. 6, pp. 1500–1504, 2019. DOI: 10.1002/mop.31799.

[3] A. El Mostrach, A. Muller, J.-F. Favennec, B. Potelon, A. Manchec, E. Rius, C. Quendo, Y. Clavet, F. Doukhan, and J. Le Nezet, "An RF-MEMS-based digitally tunable SIW filter in X-band for communication satellite applications", *Applied Sciences*, vol. 9, no. 9, p. 1838, 2019. DOI: 10.3390/app9091838.

[4] A. Kumari, D. Kumar, and A. Kumar, "Dual-band substrate integrated waveguide (SIW) band pass filter for scientific radar applications", *International Journal of Information Technology*, vol. 11, pp. 875–878, 2019. DOI: 10.1007/s41870-017-0076-x.

[5] D. Deslandes and K. Wu, "Integrated microstrip and rectangular waveguide in planar form", *IEEE Microwave and Wireless*

Components Letters, vol. 11, no. 2, pp. 68–70, 2001. DOI: 10.1109/7260.914305.

[6] I. Mohamed and A. Sebak, "Broadband transition of substrate-integrated waveguide-to-air-filled rectangular waveguide", *IEEE Microwave and Wireless Components Letters*, vol. 28, no. 11, pp. 966–968, 2018. DOI: 10.1109/LMWC.2018.2871330.

[7] C. T. Bui, P. Lorenz, M. Saglam, W. Kraemer, and R. H. Jansen, "Investigation of symmetry influence in substrate integrated waveguide (SIW) bandpass filters using symmetric inductive posts", in *Proc. of the 38th European Microwave Conference*, 2008, pp. 492–495. DOI: 10.1109/EUMC.2008.4751496.

[8] A. Deleniv and S. Gevorgian, "Design of the compact band-pass filter utilizing dielectric loaded waveguide resonators", in *Proc. of 2007 European Microwave Conference*, 2007, pp. 886–889. DOI: 10.1109/EUMC.2007.4405335.

[9] S. Moitra and P. S. Bhowmik, "Design and analysis of 150° bend SIW and corrugated SIW bandpass filter with multiple transmission zeroes using reactive periodic structures suitable for microwave integrated circuits (MICs)", *Wireless Personal Communication*, vol. 101, no. 1, p. 167–180, 2018. DOI: 10.1007/s11277-018-5681-x.

[10] X. Zhang, J. Yan, H. Zhang, and Y. Chen, "Miniaturized substrate integrated waveguide 5G LTCC bandpass filter exploiting capacitive loaded cavities", *Int. J. RF Microw. Comput.-Aided Eng.*, vol. 29, no. 7, p. e21730, 2019. DOI: 10.1002/mmce.21730.

[11] F. Wang, V. F. Pavlidis, and N. Ju, "Miniaturized SIW bandpass filter based on TSV technology for THz applications", *IEEE Transactions on Terahertz Science and Technology*, vol. 10, no. 4, pp. 423–426, 2020. DOI: 10.1109/TTHZ.2020.2974091.

[12] A. R. Azad and A. Mohan, "Substrate integrated waveguide cross-coupled bandpass filter with wide-stopband", in *Proc. of 2020 URSI Regional Conference on Radio Science (URSI-RCRS)*, 2020, pp. 1–4. DOI: 10.23919/URSIRCRS49211.2020.9113516.

[13] A. R. Azad and A. Mohan, "Single- and dual-band bandpass filters using a single perturbed SIW circular cavity", *IEEE Microwave and Wireless Components Letters*, vol. 29, no. 3, pp. 201–203, 2019. DOI: 10.1109/LMWC.2019.2893379.

[14] O. I. Hussein *et al.*, "Substrate integrated waveguide bandpass filtering with Fourier-varying via-hole walling", *IEEE Access*, vol. 8, pp. 139706–139714, 2020. DOI: 10.1109/ACCESS.2020.3012994.

[15] Y. Xiao, P. Shan, Y. Zhao, H. Sun, and F. Yang, "Design of a W-band GaAs-based SIW chip filter using higher order mode resonances", *IEEE Microwave and Wireless Components Letters*, vol. 29, no. 2, pp. 104–106, 2019. DOI: 10.1109/LMWC.2018.2890265.

[16] H.-R. Zhu, X.-Y. Ning, Zh.-X. Huang, and X.-L. Wu, "An ultra-compact on-chip reconfigurable bandpass filter with semi-lumped topology by using GaAs pHEMT technology", *IEEE Access*, vol. 8, pp. 31606–31613, 2020. DOI: 10.1109/ACCESS.2020.2972932.

[17] D. M. Pozar, *Microwave Engineering*. NJ: John Wiley & Sons Inc., 2012.

[18] F. F. He, K. Wu, and W. Hong, "A wideband bandpass filter by integrating a section of high pass HMSIW with a microstrip lowpass filter", in *Proc. of 2008 Global Symposium on Milimeter Waves*, Nanjing, 2008, pp. 282–284. DOI: 10.1109/GSMM.2008.4534623.

[19] A. Vala and A. Patel, "Half-mode substrate-integrated waveguide based band-pass filter for C band application", *Microwave and Optical Technology Letters*, vol. 61, no. 6, pp. 1468–1472, 2019. DOI: 10.1002/mop.31837.

[20] A. Jubril and S. D. Nyitamen, "2GHz microstrip low pass filter design with open-circuited stub", *IOSR Journal of Electronics and Communication Engineering (IOSR-JECE)*, vol. 13, no. 2, pp. 01–09, 2018. DOI: 10.9790/2834-1302020109.

[21] Sh. Garg and R. K. Raj, "A novel bandpass substrate integrated waveguide filter for the application at K & Ka band", *International Journal of Research and Analytical Reviews*, vol. 6, no. 1, pp. 1098–1102, 2019. [Online]. Available: http://www.ijrar.org/papers/IJRAR19J1279.pdf

[22] R. Kumar and Sh. N. Singh, "Compact substrate integrated waveguide multiband band pass filter using octagonal complementary split ring resonators", *International Journal of Applied Engineering Research*, vol. 12, no. 20, pp. 10127–10133, 2017. [Online]. Available: https://www.ripublication.com/ijaer17/ijaerv12n20_127.pdf

[23] K. Güvenli, S. Yenikaya, and M. Seçmen, "Design and implementation of substrate integrated waveguide filter to work on X-band and Ku-band", in *Proc. of 9th International Conference on Ultrawideband and Ultrashort Impulse Signals (UWBUSIS)*, Odessa, Ukraine, 2018, pp. 198–200. DOI: 10.1109/UWBUSIS.2018.8520006.

[24] Sh. Mitra and D. K. Kumuda, "Stepped impedance microstrip low-pass filter implementation for S-band application", *International Journal of Latest Trends in Engineering and Technology*, vol. 5, no. 3, pp. 248–255, 2015. [Online]. Available: https://www.ijltet.org/wp-content/uploads/2015/05/35.pdf

[25] L. Zhao, Y. Li, Zh.-M. Chen, X.-H. Liang, J. Wang, X. Shen, and Q. Zhang, "A band-pass filter based on half-mode substrate integrated waveguide and spoof surface plasmon polaritons", *Sci. Rep.*, vol. 9, no. 1, 2019. DOI: 10.1038/s41598-019-50056-9.

[26] CST (Computer Simulation Technology) Studio Suite, 2017. [Online]. Available: https://www.cst.com/2017

[27] A. Merfeldas, P. Kuzas, D. Gailius, Z. Nakutis, M. Knyva, A. Valinevicius, D. Andriukaitis, M. Zilys, and D. Navikas, "An Improved Near-field Magnetic Probe Radiation Profile Boundaries Assessment for Optimal Radiated Susceptibility Pre-Mapping", *Symmetry*, vol. 12, no. 7, p. 1063, Jun. 2020. DOI: 10.3390/sym12071063..